Pacific Northwest
NATIONAL LABORATORY

PNNL-29972

Xenon Abatement Simulations to Support the KAERI Medical Isotope Facility

September 2020

David Stephenson
Charles Doll
Jim Hayes
Paul Humble
Justin McIntyre
Andrew Ritzmann

U.S. DEPARTMENT OF ENERGY

Prepared for the U.S. Department of Energy
under Contract DE-AC05-76RL01830

DISCLAIMER

PACIFIC NORTHWEST NATIONAL LABORATORY
operated by
BATTELLE
for the
UNITED STATES DEPARTMENT OF ENERGY
under Contract DE-AC05-76RL01830

Printed in the United States of America

Available to DOE and DOE contractors from the
Office of Scientific and Technical Information,
P.O. Box 62, Oak Ridge, TN 37831-0062;
ph: (865) 576-8401
fax: (865) 576-5728
email: reports@adonis.osti.gov

Available to the public from the National Technical Information Service
5301 Shawnee Rd., Alexandria, VA 22312
ph: (800) 553-NTIS (6847)
email: orders@ntis.gov <https://www.ntis.gov/about>
Online ordering: http://www.ntis.gov

PNNL-29972

Xenon Abatement Simulations to Support the KAERI Medical Isotope Facility

September 2020

David Stephenson
Charles Doll
Jim Hayes
Paul Humble
Justin McIntyre
Andrew Ritzmann

Prepared for
the U.S. Department of Energy
under Contract DE-AC05-76RL01830

Pacific Northwest National Laboratory
Richland, Washington 99354

Summary

To maintain and improve the verification regime that is outlined by the Preparatory Commission for the Comprehensive Nuclear-Test-Ban-Treaty Organization there is a need to understand and reduce the radioxenon releases from medical isotope production facilities. In support of this objective, Pacific Northwest National Laboratory (PNNL) was tasked with modeling and evaluation of the abatement process and delay bed designs for the medical isotope production facility under construction by the Korea Atomic Energy Research Institute (KAERI). This report includes the analysis and provides PNNL proposed modifications to the KAERI adsorption bed design. The specific tasks accomplished by PNNL are:

- Obtain adsorbent parameters for modeling of KAERI's adsorbent beds,
- Validation of KAERI's cooled gas trap design and determining gaps in their technology,
- Develop an optimal cooled trap model, determine operating parameters, and determine the best location for cooling a cooled trap design,
- Provide feedback and recommended design changes to KAERI about their design.

Acronyms and Abbreviations

KAERI	Korea Atomic Energy Research Institute
MI	Medical Isotopes
Bq	Becquerel
GM	Gifford McMahon
IMS	International Monitoring System
LPM	Liters Per Minute
^{99}Mo	Molybdemum-99
Nu	Nusselt Number
N_2	Nitrogen
PNNL	Pacific Northwest National Laboratory
Pr	Prandtl Number
Re	Reynolds Number
SS 4340	Stainless Steel 4340

Contents

Figures & Tables

1.0 Introduction

Production of the medical isotope Molybdenum 99 (^{99}Mo) from fission of uranium creates radioxenon as a byproduct that can interfere with nuclear explosion monitoring if released to the environment. While the unmitigated releases themselves are well below regulatory reporting requirements, they can be easily detected by the sensitive equipment used as part of the the International Monitoring System (IMS) put in place by the Preparatory Commission for the Comprehensive Nuclear-Test-Ban Treaty Organization for monitoring nuclear explosions several thousand kilometers from the point of detonation. To reduce these emissions to levels well below detection by IMS stations, producers have incorporated several engineered methods to capture or delay the release of isotopes, thus allowing them to decay to low levels. These methods include adsorption delay beds and holding tanks which are in most cases quite large and require significant radiation shielding to minimize exposure to plant operators. The size of the adsorbent bed is driven by the volume of the sequestered air and the temperature of the bed so reducing the sequestered air volume or lowering the temperature of the bed can significantly reduce the size of the adsorption beds. There is a significant drive to better understand how to minimize the size of the delay beds while maintaining all safety and abatement objectives.

Pacific Northwest National Laboratory (PNNL) has a significant history developing the monitoring systems that collect and measure radioxenon isotopes from atmospheric samples for the purposes of detecting underground nuclear explosions. This project uses that expertise to help the KAERI medical isotope production facility verify their radioxenon abatement trap design to keep the facilities releases of radioxenon to less than 5e9 Becquerel (Bq) per day which is a level of releases deemed to not have an unacceptably negative effect on international nuclear explosion monitoring. The research and development of PNNL modeling will be freely available to other medical isotope producers with the goal of fostering the worldwide reduction of radioxenon emissions from medical isotope facilities.

To help KAERI evaluate their abatement trap design, PNNL developed an adsorption model for two of KAERI's abatement trap designs and evaluated the radioxenon activity that will exit the traps after decay of 80 days in these models. PNNL included cooling from two different methods, adsorption isotherms of xenon on cold activated carbon, input flow rate, heat of adsorption, and heat of radioxenon decay in the model.

2.0 Medical Isotope Production Abatement Flow Path

A schematic of a general medical isotope (MI) abatement process is shown in Figure 1. In the typical process, effluent gases from the uranium irradiation and from the extraction process of ^{99}Mo are passed into buffer tanks where short-lived isotopes can decay. The gas from the holding tanks is then passed through decay tanks and through delay beds where radioxenon is held for typically >80 days. After 80 days, the radioxenon is decayed to low enough levels that it is acceptable to release. The delay beds used are sized primarily to handle high flow rates from the hot cell, as well as the lower concentration radioxenon coming from MI producer's decay tanks.

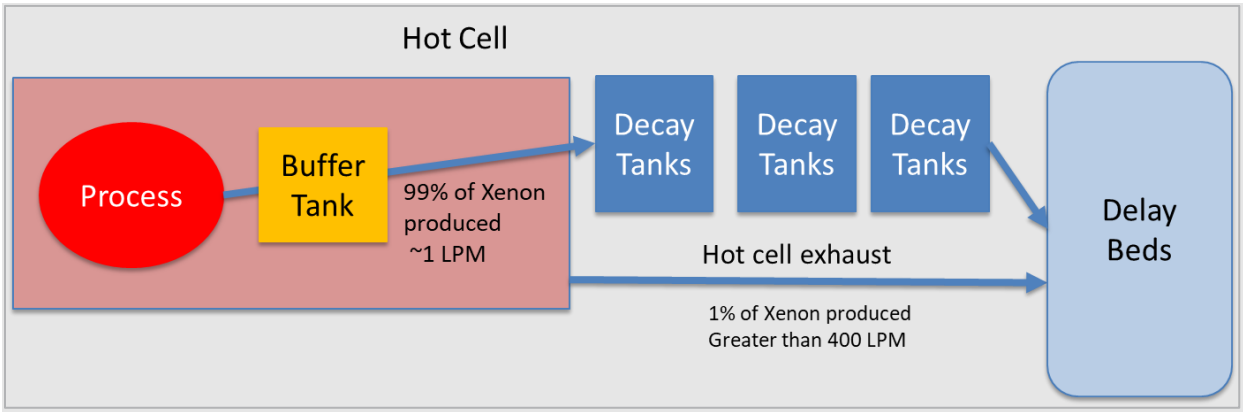

Figure 1. Typical MI abatement process using decay tanks to allow sufficient time for xenon decay.

2.1 KAERI's Proposed Abatement Flow Path

KAERI's proposed abatement process is different than the typical process as it replaces larger decay tanks with three cooled adsorbent beds that can fit within their planned hot cell design. Using cooled beds instead of ambient temperature beds allows for longer holdup on much smaller beds. Each cooled bed is to be sized so that it can handle a 0.3 l/min flow for 16 hours every 24 hours for 40 days. The lower flow rate allows for the xenon gas to move much slower through the cold bed than the ambient temperature bed. By switching the process flow between beds every 40 days, at least 80 days (or approximately five orders of magnitude reduction of ^{133}Xe) abatement of ^{133}Xe is to be achieved. A schematic of a KAERI's MI abatement process is shown in Figure 2.

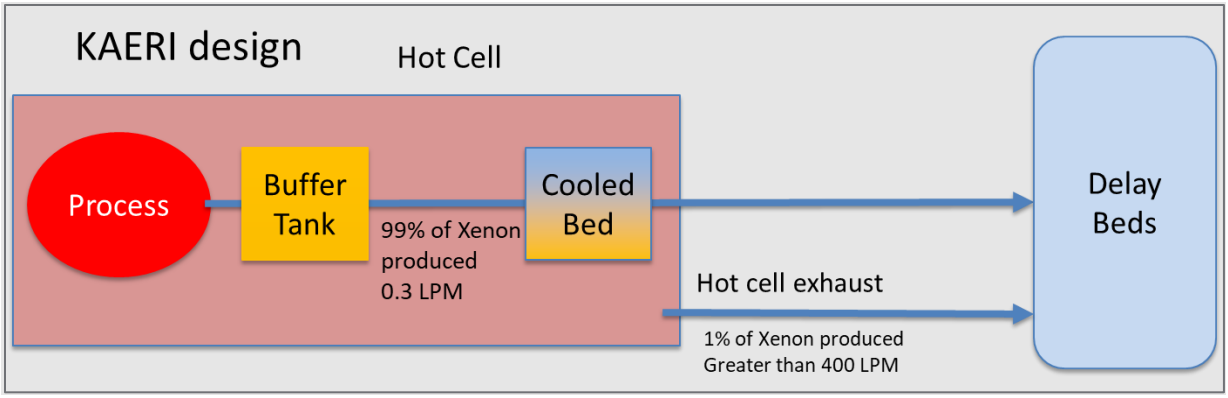

Figure 2. KAERI's proposed abatement process using a cooled bed to allow enough time for radioxenon decay.

2.2 KAERI's Bed Designs and Cooling Technologies

KAERI has proposed two different cooling technologies for the same sized cooled adsorbent bed size (84 cm long, 8.6 cm inner diameter, Figure 3), one which is cooled with liquid coolant and the other which is cooled with a mechanical cold head connected to the adsorbent trap.

The first technique uses vapor compression technology to cool a liquid (propylene glycol/water solution) that circulates around the adsorbent bed to cool the bed. The circulating coolant achieves -18 ˚C. This cooling technique has no mechanical parts inside the hot cell, should have faster re-cooling times and fewer if any issues with heat leaks. It is unknown what level of radiation activity will degrade the propylene-glycol and if the solution may need to be replaced occasionally.

Figure 3. KAERI liquid cooled adsorbent testbed.

The second technique uses cooling from a Gifford McMahon (GM) cryocooler by connecting the cold head to the bottom of a vacuum jacketed adsorbent bed (Figure 4). Xenon flows into the bottom of the adsorbent bed with a nitrogen (N_2) carrier gas. Xenon is adsorbed in the bed while nitrogen passes through. A laboratory scale version was developed by KAERI and is shown in Figure 4. The adsorbent bed using the GM cooling technique was tested by KAERI and was able to reach -105 ˚C when flowing nitrogen and stable xenon through the bed.

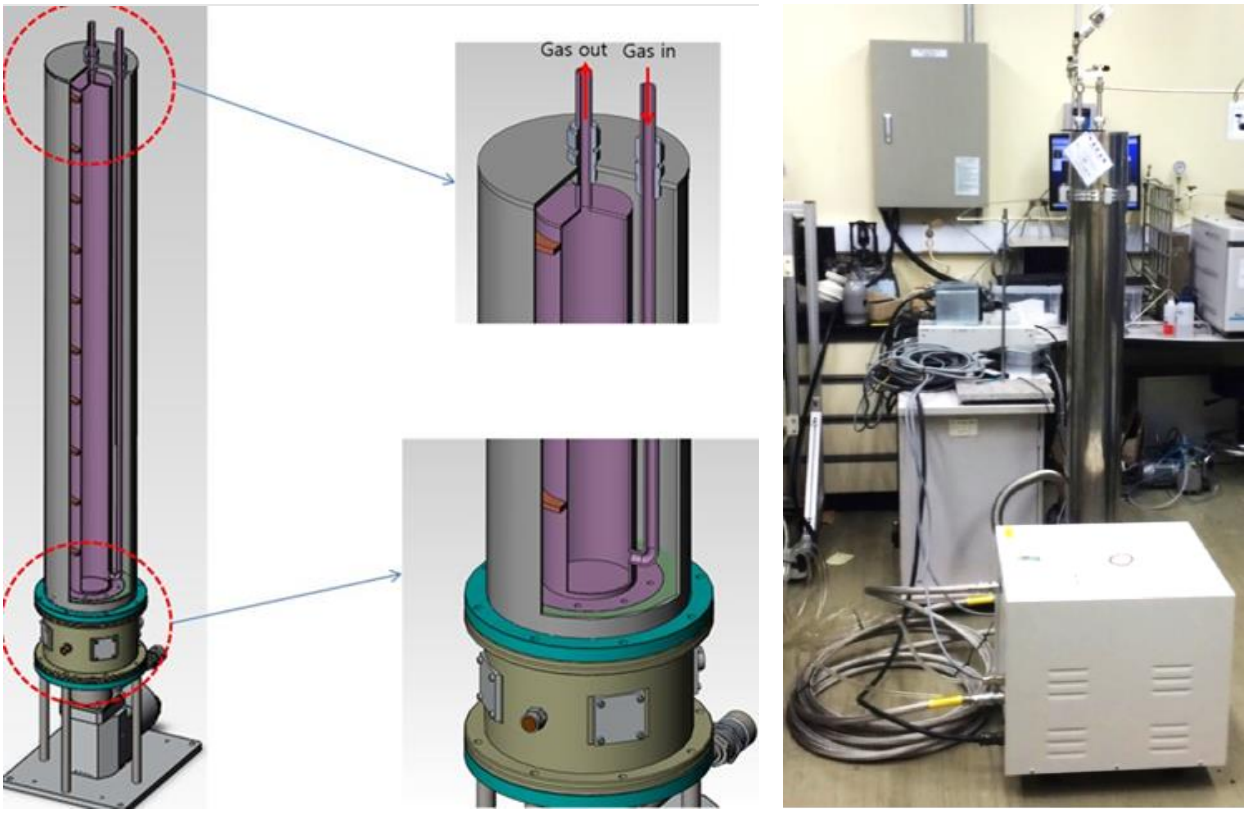

Figure 4. Images of KAERI's prototype system.

3.0 Model Equations

The following equations were implemented using a finite element modeling software called COMSOL Multiphysics. COMSOL allows for the modeling of complex bed geometries. For this case, we used a 2D axial symmetric model geometry to solve flow of gases coupled with heat transfer. The following assumptions were used in deriving the partial differential equations used in the finite element model:

- The gas phase behaves ideally
- Plug flow through the packed bed
- Thin-film mass transfer resistance is negligible
- Gravitational effects are neglected
- For modeling heat transfer the gas is assumed to be non-compressible

3.1 Gas Transport

The gas phase mass balance for each species using Darcy's law and including gas diffusion is given in equation 1 [1].

$$\varepsilon \frac{\partial c_i}{\partial t} + \nabla \cdot \left(-D_{igas} \nabla c_i - c_i \frac{\kappa}{\mu} \nabla \left(RT \sum_{j=1}^{n} c_j \right) \right) = -R_i - \lambda_i c_i \quad (1)$$

In this equation, c_i is the gas phase concentration of species i, ε is the bed porosity, κ is the permeability of the solid phase, μ is gas viscosity, R is the ideal gas constant, and T is the temperature. The term D_{igas}, is an effective diffusion coefficient that accounts for all axial dispersion effects. R_i is the rate of adsorption (mass transfer from the gas to the solid adsorbent) and λ_i is the first order decay constant used to model radioactive decay of species i. The permeability of the packed bed was estimated using the empirical equation (equation 2) developed by Rumpf and Gupte [2] as written by Nirschl and Schäfer [3].

$$\kappa = \frac{\varepsilon^{5.5}}{5.6} d_p \quad (2)$$

In equation 2, ε is the bed porosity and d_p is the characteristic diameter of the particles in the packed bed.

3.2 Adsorption

Adsorbed phase mass balance for each species is given in equation 3 where $c_{i,ad}$ is the concentration of species i on the adsorbent R_i is the rate of adsorption and λ_i is the first order decay constant used to model radioactive decay.

$$\frac{\partial c_{i,ad}}{\partial t} = R_i - \lambda_i c_{i,ad} \quad (3)$$

The rate of mass transfer between the gas and adsorbed phase is based on a competitive Langmuir adsorption isotherm using the linear driving force approximation (equation 4).

$$R_i = K_i \cdot \left[\frac{\rho_b N_{io} b_i(T) RT c_i}{1 + \sum_j b_j(T) RT c_j} - c_{i,ad} \right] \quad (4)$$

In this equation, K_i is the mass-transfer coefficient of species *i*, , ρ_b is the packed bed density, N_{io} is the saturation capacity of the adsorbent, b_i is the Langmuir constant [4] for species *i* with the adsorbent (obtained using equation 5 below), c_i is the concentration of species *i* in the gas phase and $c_{i,ad}$ is the concentration of species *i* in the adsorbed phase.

$$b_i = b_{io} e^{Q_i/RT} \quad (5)$$

Q_i is the heat of adsorption for species i on the adsorbent.

We are assuming that the mixture components have the same saturation capacity [5] on a given adsorbent. In addition, simple calculations were performed in Microsoft Excel with a competitive Langmuir adsorption isotherm approach (N_2 and Xe species) to determine the expected hold up times of the KAERI beds. These calculations are at constant flowrates, rather than the variable flowrates proposed by KAERI and without radioxenon heating.

3.2.1 Adsorption Isotherm Data

Pure gas adsorption isotherms for gases present in air were measured at different temperatures for the NUCON GXK-6X12 activated carbon adsorbent and are shown in Figure 5. NUCON GXK-6X12 carbon is a 6X12 (3.36 mm-1.68 mm) U.S. mesh sized particles of activated carbon made from coconut shell carbons that have been activated. NUCON's Technical Bulletin 11B10 describes the properties of NUCON's activated carbons.

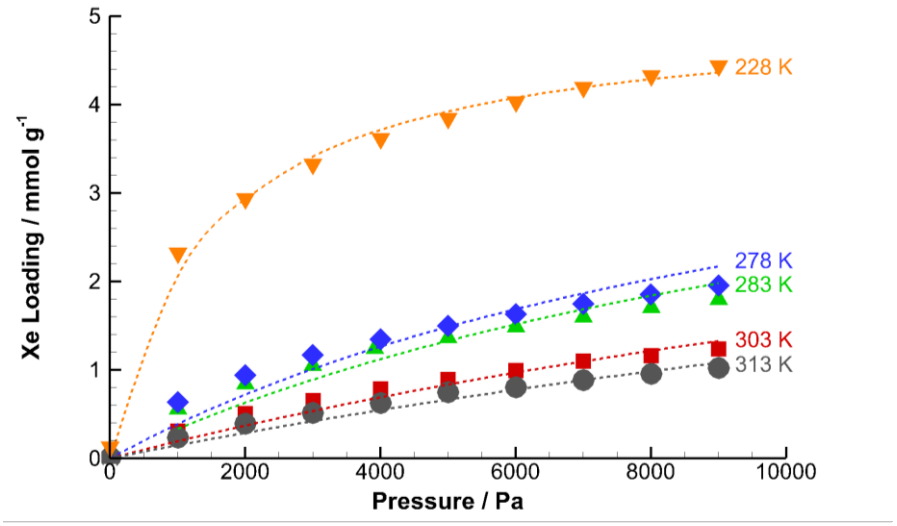

Figure 5. Plots of NUCON GXK-6X12 adsorbent isotherm data.

KAERI provided xenon breakthrough data on a similar activated carbon material manufactured by NUCON called NUSORB G30-6X12. Their data was obtained using a 0.15% Xe/N_2 carrier composition at 300 mL/min with stable xenon only. To fit the breakthrough data as shown in Figure 6 required changes to two of the adsorption model's parameters. The heat of adsorption of xenon was increased by 6.5% from 21,078 J/mol to 22,446 J/mol and the axial dispersion parameter was reduced from 1.5e-5 m^2/s [6] to 2e-6 m^2/s.

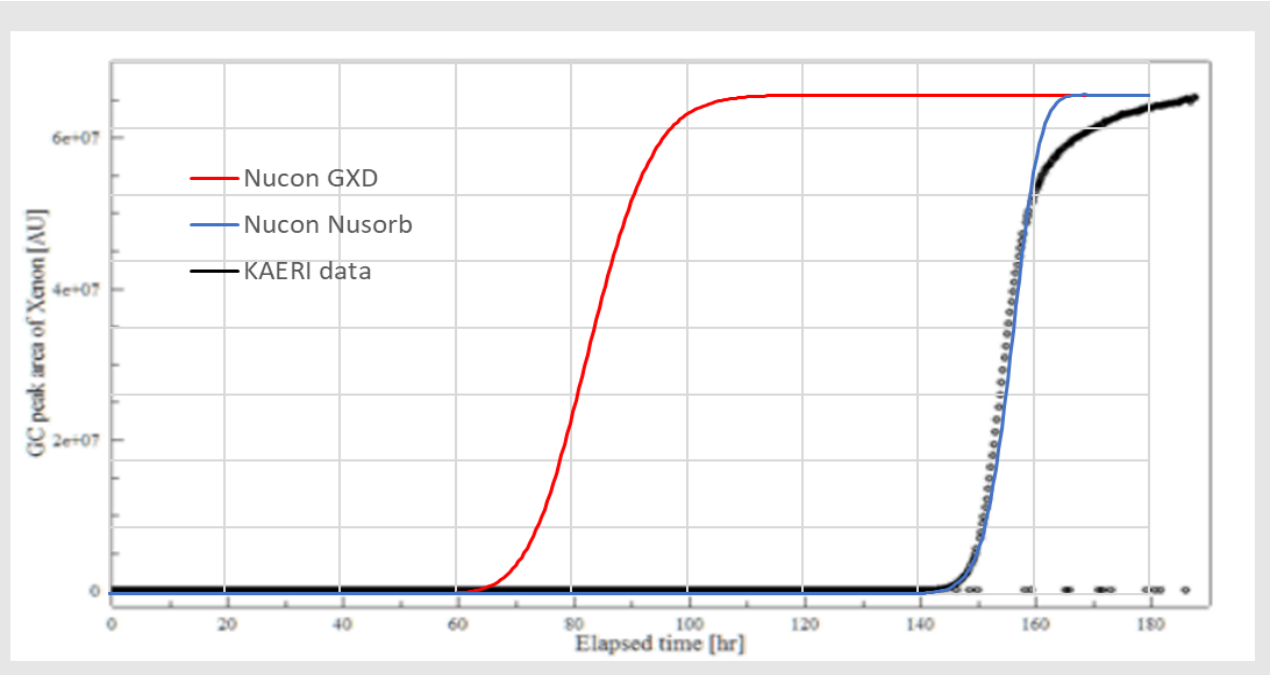

Figure 6. KAERI breakthrough data with simulations of NUCON's GXK and NUSORB materials overlaid on the experimental data.

The Langmuir constants determined from fitting the experimental data for the NUCON GXK-6x12 and the NUCON NUSORB G30-6X12 materials are shown in Table 1.

Table 1. Langmuir constants used in simple bed size calculations for NUCON GXK-6X12 and NUSORB 630-6X12 carbon materials

Bed material	Gas	N_o (mol/g)	B_o (1/Pa)	Q_{ad} (J/mol)
NUCON GXK-6x12	Xenon	0.00593	9.09E-09	21100
NUCON GXK-6x12	Nitrogen	0.00593	2.57E-10	19000
NUCON NUSORB G30-6X12	Xenon	0.00593	9.09E-09	22400
NUCON NUSORB G30-6X12	Nitrogen	0.00593	2.57E-10	19000

3.3 Heat Transfer

Convection-conduction equations were developed to model heat transfer in the adsorption bed. Separate equations were developed for the gas and adsorbent phases and a heat transfer coefficient was used to model heat transfer between the gas and solid phase. Equation 6 shows the heat transfer equation used for the gas phase.

$$\rho_g Cp_g \frac{\partial T_g}{\partial t} + \rho_g Cp_g \overrightarrow{u_g} \nabla T_g + \nabla \cdot \left(-k_g \nabla T_g\right) = q_{\text{decay,i}} + ah\left(T_b - T_g\right) \quad (6)$$

In this equation, T_b is the adsorbent temperature, T_g is the temperature of the gas, and $\overrightarrow{u_g}$ is the velocity of the gas as described by Darcy's flow from equation 1, the parameter Cp_g is the heat capacity of the gas, k_g is the thermal conductivity of the gas, $q_{\text{decay,i}}$ is the heat generated by radioactive decay described below, a is the specific surface area of the bed, and h is heat transfer coefficient for the bed particles. This equation assumes that the gas density is constant (incompressible flow) despite the compressibility of gases. However, this approximation is reasonable in the regime of relatively small temperature changes.

The conduction equation in the adsorption bed for the solid adsorbent phase is given in equation 7.

$$\rho_b Cp_b \frac{\partial T_b}{\partial t} + \nabla \cdot (-k_b \nabla T_b) = q_{\text{decay,i}} - ah(T_b - T_g) \quad (7)$$

In this equation, Cp_b is the heat capacity of the bed and k_b is the thermal conductivity of the bed. The other parameters and variables appearing in this equation are as previously described.

3.4 Radioactive Decay

Atoms undergoing radioactive decay release large amounts of energy. We assume that the decay energy is the difference between the ground states of the parent and daughter nuclei. Xenon-133 and ^{135}Xe undergo β decay to form ^{133}Cs and ^{135}Cs, respectively and 427.4 keV (4.12×10^{10} J/mol) and 1165 keV (1.12×10^{11} J/mol) are emitted from the decay of these isotopes respectively. [7, 8] As β-decay is the primary mechanism, we treat the decay energy in a local manner to keep the problem tractable. Radioactive decay is a first-order process and equation 8 defines the associated heat generation term ($q_{\text{decay,i}}$) for isotope i.

$$q_{\text{decay,i}} = \lambda_{\text{i}} c_{\text{i}} Q'_{\text{i}} \quad (8)$$

In Equation 8, $c_{,i}$ is the concentration (in mol/m^3) of the radioxenon species (this is the gas phase concentration for equation 6, and the adsorbed gas concentration for equation 7), λ_i is the first order decay constant for the species, and Q'_i is the decay energy in J/mol for the species.

3.5 Model Parameters

Many of the model parameters are available from the problem specification or in peer-reviewed sources. For instance, little uncertainty remains in the measurable properties of air. These known model parameters are reported in Table 2.

Table 2. Model parameters obtained from problem specification (no source provided) or from the literature.

Quantity	Parameter Definition	Value	Source and Notes
$\dot{V}$	Volumetric Flow Rate	0.3 L/min	For 16 hours per 24 hours
L	Bed Length	0.84 m	84 cm
r	Bed Radius	0.084 m	8.4 cm
ε	Porosity	0.43	Assumed
d_p	Diameter of Particle	0.001285 m	Assumed
$C_{p,g}$ (300 K, 1 atm)	Heat Capacity, gas	1006 J/kg*K	[9] pg. 41
ρ_g (300 K, 1 atm)	Density, gas	1.177 kg/m^3	[9] pg. 35
k_g (300 K, 1 atm)	Thermal Conductivity, gas	0.02624 W/m*K	[9] pg. 70
μ_g (300 K, 1 atm)	Viscosity, gas	1.85 × 10^{-5} Pa*s	[9] pg. 69
Pr_g (300 K, 1 atm)	Prandtl number, gas	0.708	[9] pg. 71
k_b	Thermal Conductivity, bed	0.20 W/m*K	[10] states typical values are between 0.17 and 0.27 W/m*K
h	Heat transfer coefficient	102 W/m^2*K	See below
$C_{p,b}$	Heat Capacity, bed	770 J/kg*K	[11]
ρ_b	Density, bed	645 kg/m^3	(Measured for Alamo activated carbon sample)
$\lambda_{^{131m}Xe}$	Decay Constant, ^{131m}Xe	6.78 × 10^{-7} s^{-1}	[7, 12] [1]
$Q'_{^{131m}Xe}$	Decay Heat, ^{131m}Xe	1.58 × 10^{10} J/mol	[12, 13]
$\lambda_{^{133}Xe}$	Decay Constant, ^{133}Xe	1.53 × 10^{-6} s^{-1}	[7, 12][1]
$Q'_{^{133}Xe}$	Decay Heat, ^{133}Xe	4.12 × 10^{10} J/mol	[7, 12]
$\lambda_{^{135}Xe}$	Decay Constant, ^{135}Xe	2.11 × 10^{-5} s^{-1}	[8, 12][1]
$Q'_{^{135}Xe}$	Decay Heat, ^{135}Xe	1.12 × 10^{11} J/mol	[8, 12]
N_{Xeo}	Saturation Capacity, Xe	5.11× 10^{-3} mol/gm	Fit from data (figure 1)
Q_{Xe}	Heat of Adsorption, Xe	21080 J/mol	Fit from data (figure 1)
B_{Xeo}	Langmuir Constant, Xe	9.09× 10^{-9} 1/Pa	Fit from data (figure 1)

N_{N2o}	Saturation Capacity, N_2	1.03× 10^{-2} mol/gm	Fit from data of typical activated carbon + breakthrough experiments
Q_{N2}	Heat of Adsorption, N_2	19000 J/mol	Fit from data of typical activated carbon + breakthrough experiments
B_{N2o}	Langmuir Constant, N_2	2.57× 10^{-10} 1/Pa	Fit from data of typical activated carbon + breakthrough experiments
[1] Decay constants (λ_i) are related to the isotopic half-lives ($\lambda_i = \ln(2)/t_{1/2,i}$)			

The heat transfer coefficient (*h*) between activated carbon and air depends on the physical behavior of the fluid flow through the bed. Correlations between dimensionless groups (*e.g.*, *Nusselt (Nu)*, *Reynolds (Re)*, and *Prandtl (Pr) numbers*) have been developed and are available in the literature that allow estimation of the heat transfer coefficient. In our case, we employ the correlation (Equation 9) developed by Gunn [14] to estimate the value of *h*.

$$Nu = (7 - 10\varepsilon + 5\varepsilon^2)(1 + 0.7Re^{0.2}Pr^{\frac{1}{3}}) + (1.33 - 2.4\varepsilon + 1.2\varepsilon^2)Re^{0.7}Pr^{\frac{1}{3}} \quad (9)$$

We estimate that for the process we are simulating *h* = 102 W/m^2*K at 300 K and 1 atm. The specific surface area per unit volume using is calculated using equation 10 [14].

$$S = \frac{6(1-\varepsilon)}{d_{\mathrm{p}}} \quad (10)$$

Quantifying emissions requires converting the number of moles (or atoms) of radioxenon isotopes into a measurable radioactivity (in Bq). The instantaneous emission rate of isotope i ($\dot{E}_{\mathrm{I}}$) is derived from the outlet concentration via the relationship

$$\dot{E}_{\mathrm{I}}(t) = c_{\mathrm{i,out}}(t)\dot{V}N_{\mathrm{A}}\lambda_{\mathrm{i}} \quad (11)$$

where N_A is Avogadro's number (6.022 × 10^{23} atoms/mole), $c_{i,out}$ is the outlet concentration of isotope , and $\dot{V}$ is the volumetric flow rate. The units of $\dot{E}_{\mathrm{I}}$ are Bq/s which can easily be converted into Bq/day. If multiple isotopes are present, then the emissions rate becomes a sum over all the isotopes present.

4.0 Modeling Results Vapor Compression

PNNL modeled the effectiveness of the vapor compression cooling method using our COMSOL model (Table 3). The goal was to evaluate radioxenon holdup on the adsorbent beds for each method to determine if bed length, diameter, and flow rate achieved the 40-day expected holdup. For the baseline cooling profile, KAERI measured a uniform temperature along the adsorbent bed when testing their prototype system.

PNNL modeled breakthrough times using KAERI's proposed adsorbent bed size, cooling temperatures, and flow conditions to evaluate the effectiveness for holding radioxenon. The results are shown in Table 3 with and without radioxenon heat of decay.

Table 3. COMSOL Multiphysics simulations with and without radioxenon heating.

COMSOL Multiphysics modeling of cooled bed (-18 deg C) with variable flowrate but no radioxenon heating					
Model	Flow (LPM)	Flow conditions	Radioxenon heat of decay	Cooling conditions	Breakthrough time (1e9 Bq/day)
COMSOL	0.3	16 hr/day	no heat of decay	-18 °C	27 days
COMSOL	0.3	16 hr/day	$^{133}Xe+^{135}Xe$	-18 °C	24 days
Excel	0.2	24 hr/day	No heat of decay	-18 °C	40 days

For flow conditions of 0.3 LPM, the holdup times do not reach the expected 40 days. With no radioxenon heat of decay, the holdup time was calculated to be 27 days, and with radioxenon heat of decay the holdup was calculated to be 24 days. To achieve a 40-day holdup time according to a simplified Excel model, the flow rate needs to be an average of 0.2 LPM at -18° C.

Figure 7 shows the trap temperature profile and the radioxenon emissions as a function of time (40 days of 16 hr/day) for the vapor compression cooling bed. The maximum temperature differential in the bed is 42 ˚C above the flowing -18 ˚C cooling fluid, however, the average bed temperature is -4.2 ˚C throughout the bed.

The emission performance of the vapor compression cooled bed over 40 days of delay time, and subsequent restart after another 40 days is shown in Figure 7 below.

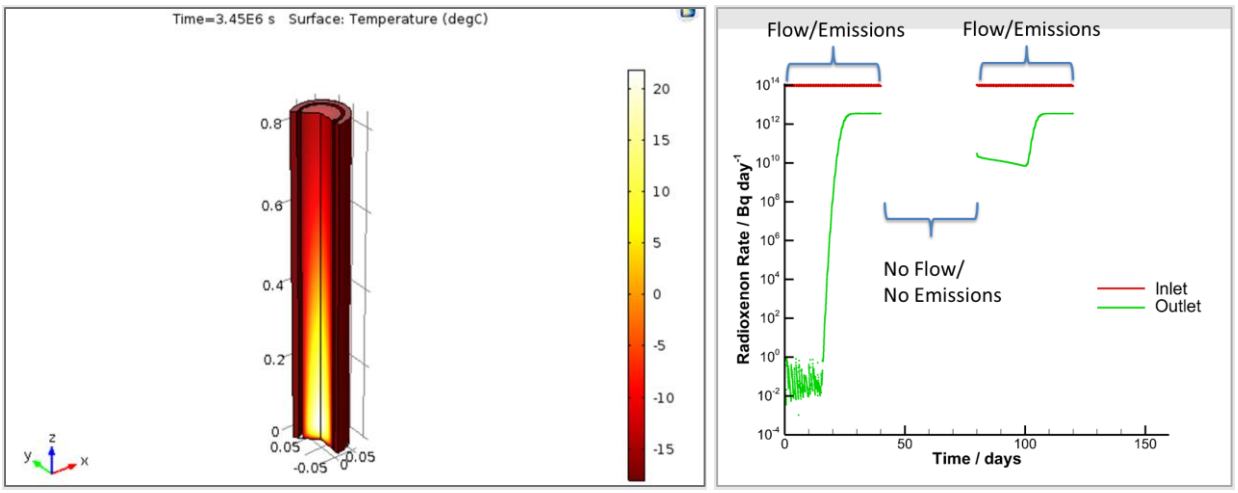

Figure 7. Temperature profile of the vapor compression cooled bed after 40 days of radio-xenon abatement (left). Radioxenon emissions as a function of time for vapor compression cooled bed (right).

Figure 7 (right figure) shows the expected radioxenon activity concentration release after 40 days of flow at 0.3 LPM. Under these conditions, the release is calculated to be ~1e13 after 40 days. Figure 7 also show that after 40 days of no flow through the adsorbent bed, and subsequent startup of 0.3 LPM, the radioxenon activity is still 1e10 Bq/day exiting the adsorbent bed and after 24 days from restart, radioxenon activity levels return to ~1e13 Bq/day which is a 1X abatement level not the 5X abatement level target.

5.0 PNNL Proposed Changes to KAERI's Vapor Compression Cooled Bed Design

PNNL calculated that increasing the bed length to 136 cm long while keeping the same 8.6 cm ID or changing the bed diameter to 12 cm ID with the original bed length of 84 cm is sufficient to reduce radioxenon emissions to 1e9 Bq/day using a vapor compression cooled liquid bed. For the longer length bed (136 cm) the required adsorbent bed volume is 7.9 liters of activated carbon. However, increasing the bed diameter causes reduced heat transfer making the bed temperature rise. This means the 12 cm ID bed design requires a larger volume of 9.5 liters. These results are shown in Figure 8.

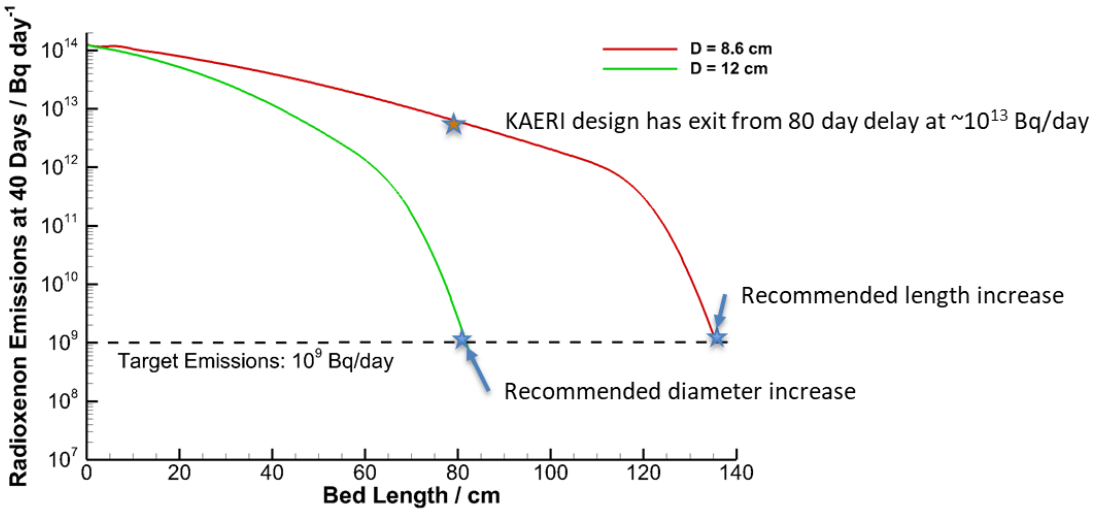

Figure 8. PNNL proposed changes to KAERI's vapor compression cooled design and subsequent radioxenon emission levels.

PNNL also calculated that with the adsorbent bed size changes, the radioxenon activity concentration after 40 days of processing is <1e9 Bq/day. After a 40-day hold time and restart and another 40 days of processing, the activity concentration remains below 1e9 Bq/m^3. See Figure 9 below.

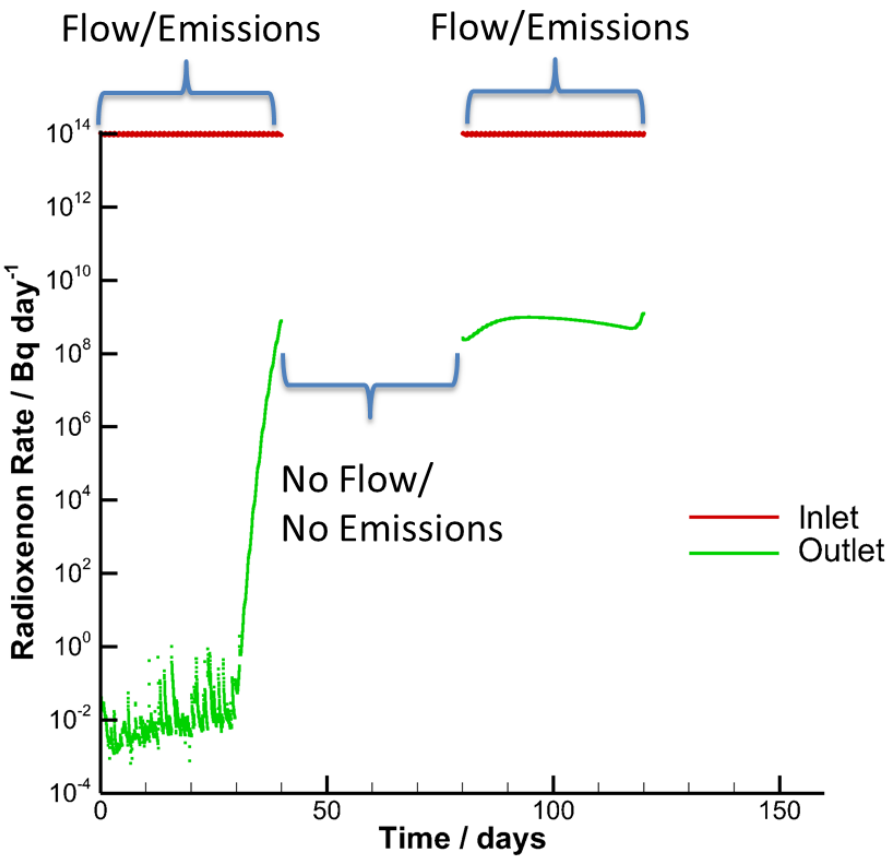

Figure 9. Radioxenon activity concentration after 40 days of processing, 40 days of hold, and another 40 days of processing on the proposed 136 cm x 8.6 cm ID bed.

6.0 Modeling Results for GM Cryocooled Adsorbent Bed

PNNL also modeled the effectiveness of the Gifford McMahon cooling method using the same conditions as the vapor compression method. For these calculations, PNNL used KAERI's testbed data in addition to the PNNL COMSOL model. KAERI measured a temperature variation of 68 ˚C along the adsorbent bed when testing their prototype system. Using the temperature profile of 68 ˚C PNNL calculate the heat losses on the top of the trap of ~9W. The calculations were performed with the estimated trap wall thickness of 8 mm thick stainless steel (SS 4340).

Figure 10 shows simulated temperature profiles after 40 days of abating the radioxenon which show a 110 ˚C rise in temperature from the cold heads -105 ˚C. This simulation is a best-case scenario that allows for the cold head to provide all the needed cooling power. The bottom of the trap achieves optimal temperature of -105 ˚C, however, the top of the adsorbent bed can only achieve 5 ˚C. An optimal cooling profile would have the full trap equilibrated at -105 ˚C.

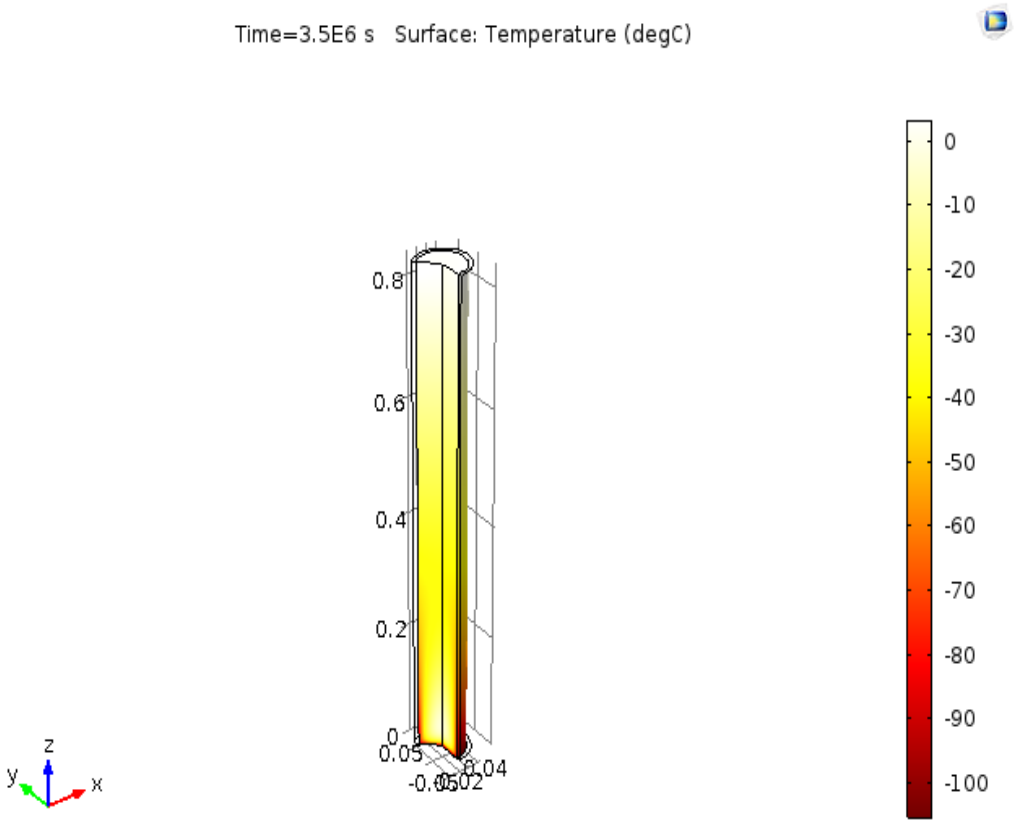

Figure 10. Temperature profile of the cryocooled bed after 40 days of radioxenon abatement.

The modeling results shown in **Error! Reference source not found.** suggested enough delay time could be achieved by using the mechanically cooled adsorbent bed.

Table 4. COMSOL Multiphysics modeling of KAERI vapor compression cooled bed with variable flow conditions with radioxenon heating and end of bed cooled to -105 ºC.

Model	Flow (LPM)	Flow Conditions	Heating Conditions	Cooling Conditions	Breakthrough time (1e9 Bq/day)
COMSOL	0.3	16hr/day	$^{133}Xe+^{135}Xe$	-105 °C	61 days

Radioxenon emissions as a function of bed length at 40 days of delay time is shown in Figure 11.

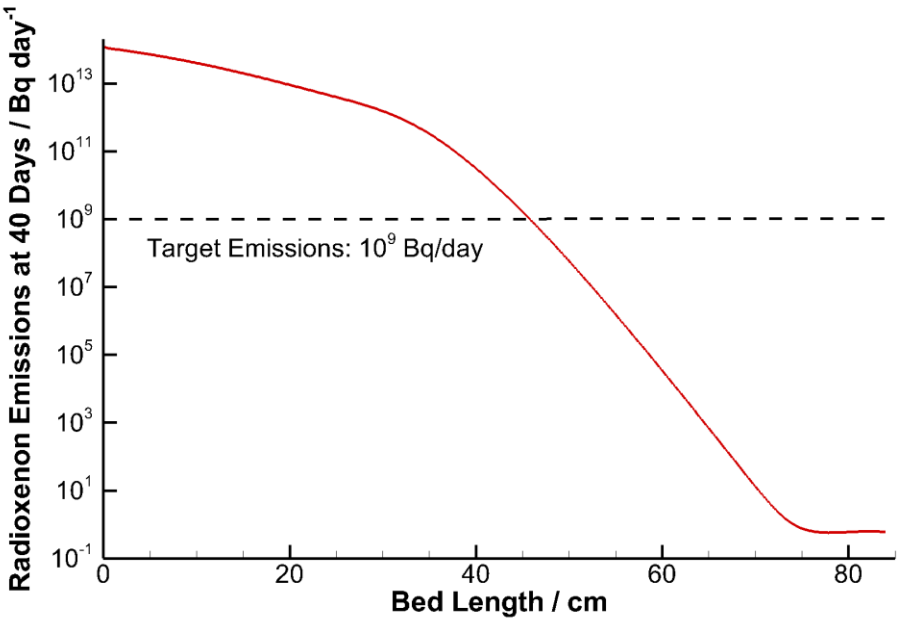

Figure 11. Radioxenon level versus bed length at 40 days of delay time for KAERI cryocooled bed.

While the cryocooled bed appears to have enough abatement time for the proposed and tested design, there are more design challenges for this cooling method that should be considered. One of these design challenges may include mitigating heat loss through possible heat leaks at the top of the trap.

7.0 Conclusions

KAERI's modeling and designs are very good but need to consider heat of decay and variable flowrates and their effects on the abatement process. Flowrate into adsorbent beds are the largest consideration for bed sizing. Lower flow rates improve retention times significantly. Heat transport is an issue at low flowrates (i.e. less than 10 LPM). Heat of radioxenon decay will require larger beds than bed estimations performed without heating effects. Cooled adsorbent beds can significantly reduce bed sizes but cooling is the most effective at low flowrates.

Vapor compression

PNNL recommends KAERI either lengthens their vapor compression cooled column(s) or increases the diameter of their proposed columns. Increasing the bed length to 136 cm long, keeping the same 8.6 cm ID or changing the bed diameter to 12 cm ID with the original bed length of 84 cm is sufficient to reduce radioxenon emissions to 1e9 Bq/day using a vapor compression cooled liquid bed. For the longer length bed (136 cm) the required adsorbent bed volume is 7.9 liters of activated carbon. However, increasing the bed diameter causes reduced heat transfer making the bed temperature rise. This means the 12 cm ID bed design requires a larger volume of 9.5 liters of activated carbon.

Maintenance for the vapor compression cooled system will likely be replacement of cooling fluid due to radiation damaging the coolant. Possible radiation testing of different liquid coolants would help quantify their susceptibility to radiation damage.

Mechanically cooled column

PNNL has determined that there are several challenges with implementation of a mechanically cooled adsorbent trap design.

- Cryopumps will need to have at least 63W (~54W from radioactive species decay) of cooling lift at the desired cooling temperature;
- The maintenance of mechanical cold head parts inside the hot cell may be challenging;
- In case of power outages there will be longer delay times to re-cool beds;
- Heat leaks will be important to mitigate given ~9W of a heat leak caused a 68 ˚C temperature rise.

8.0 References

Biblography

1. Jin, X., A. Malek, and S. Farooq, *Production of Argon from an Oxygen−Argon Mixture by Pressure Swing Adsorption.* Industrial & Engineering Chemistry Research, 2006. **45**(16): p. 5775-5787.
2. Rumpf, H. and A.R. Gupte, *Influence of Porosity and Particle Size Distribution in Resistance Law of Porous Flow.* Chemie Ingenieur Technik, 1971. **43**(6): p. 367-375.
3. Nirschl, H. and B. Schäfer, *Distinction between electrostatic and electroviscous effects on the permeability of colloidal packed beds.* Chemical Engineering & Technology, 2005. **28**(8): p. 862-866.
4. Yang, R.T., *Gas Separation By Adsorption Processes*. Series on Chemical Engineering. Vol. 1. 1997, London: Imperial College Press.
5. Rao, M.B. and S. Sircar, *Thermodynamic Consistency for Binary Gas Adsorption Equilibria.* Langmuir, 1999. **15**(21): p. 7258-7267.
6. Edwards, M.F. and J.F. Richardson, *Gas Dispersion in Packed Bed.* Chemical Engineering Science, 1968. **23**: p. 109–123.
7. Khazov, Y., A. Rodionov, and F.G. Kondev, *Nuclear Data Sheets for A=133.* Nuclear Data Sheets, 2011. **112**(4): p. 855-1113.
8. Singh, B., A.A. Rodionov, and Y.L. Khazov, *Nuclear data sheets for A=135.* Nuclear Data Sheets, 2008. **109**(3): p. 517-698.
9. Hilsenrath, J., et al., *Circular of the Bureau of Standards no. 564: Tables of Thermal Properties of Gases Comprising Tables of Thermodynamic and Transport Properties of Air, Argon, Carbon Dioxide, Carbon Monoxide, Hydrogen, Nitrogen, Oxygen, and Steam*. 1955: U.S. Department of Commerce: National Bureau of Standards. 488.
10. Kuwagaki, H., et al., *An improvement of thermal conduction of activated carbon by adding graphite.* Journal of Materials Science, 2003. **38**(15): p. 3279-3284.
11. Lutcov, A.I., V.I. Volga, and B.K. Dymov, *Thermal Conductivity, Electric Resistivity and Specific Heat of Dense Graphites.* Carbon, 1970. **8**(6): p. 753-760.
12. Sonzogni, A. *NuDat 2.7*. 2018 [cited 2018 November 14]; Available from: https://www.nndc.bnl.gov/nudat2/.
13. Khazov, Y., I. Mitropolsky, and A. Rodionov, *Nuclear data sheets for A=131.* Nuclear Data Sheets, 2006. **107**(11): p. 2715-2930.
14. Gunn, D.J., *Transfer of Heat or Mass to Particles in Fixed and Fluidized-Beds.* International Journal of Heat and Mass Transfer, 1978. **21**(4): p. 467-476.

Appendix

The following simple model gave slightly higher heat power results in comparison to those calculated with finite element model in COMSOL. Analyzing the heat generation in a packed bed used for adsorbing radioxenon may be bounded by assuming that the bed is 100% efficient at allowing this isotope to decay. Differences between the two models were the result of the COMSOL model allowing radioactive xenon to escape the bed after the bed's delay time, while the simple model assumes all the xenon decays in the bed. The calculations below were performed using the activities provided by KAERI which were 2620 Ci of ^{133}Xe and 1040 Ci of ^{135}Xe every 24 hrs.

This approximate model makes the assumption that no radioxenon escapes the bed. Thus, it provides an upper bound to the rate of heat generation on the bed. The distribution of the radioxenon in the bed is not considered, so the models provide an estimate of the total power in the bed at a given time. Several models are used in this report to reflect different assumptions surrounding the process that KAERI employs.

Variables are defined in section 3 of this report. Relevant model parameters are provided in section 4 of this report. Namely, the activities of each isotope immediately after the dissolution process, the number of atoms of each isotope corresponding to their reported activities, the half-lives of these isotopes, and the decay energies (both ground state to ground state and average beta decay energies).

^{133}Xe and ^{135}Xe Added Daily

The simple model makes four key assumptions:

- The ^{133}Xe and ^{135}Xe isotopes are the only important species contributing to the overall bed heating;
- The ^{133}Xe and ^{135}Xe are added in bulk directly from the dissolution process to the column. There is no delay time to attenuate the activities applied to the bed;
- The ^{133}Xe and ^{135}Xe are injected instantaneously at the start of the day;
- The decay event produces the energy corresponding to the ground-state to ground-state transition of ^{133}Xe à ^{133}Cs and ^{135}Xe à ^{135}Cs.

Equations

Isotopic decay and injection (i = ^{133}Xe and ^{135}Xe):

$$N_i(t) = N_i(t_0)e^{-\lambda_i(t-t_0)} + N_{i,injected}\delta(t - n * 24\ hr)$$

The analytical form for decay over a period of time is used to make the discontinuities at the injection times possible to handle. The δ is the Kronecker delta function and *n* is any integer. In this case, it is used to ensure that the injection occurs at a 24-hour interval. t_0 is the time at the previous time step in the simulation. The model was integrated using 60 second time steps.

Energy Generation Rate:

$$P_{bed} = \sum_{i} +\lambda_i N_i(t) Q_{i,GS-GS}$$

The decay energy is taken to be the ground-state to ground-state decay energy. Conceptually, this assumption means that all β and γ energy is retained within the bed.

Simple model results

Figure 12 illustrates that the radioxenon decay heating levels off below 55 W after about 40 days. Including ^{135}Xe increases the maximum and average power generated in the bed. The effect is most significant at the injection time because the amount of ^{135}Xe is highest at this point. The ^{135}Xe decays away far faster than the ^{133}Xe, so it produces a declining amount of power as the day progresses.

This simulation provides a reasonable facsimile of the COMSOL model before breakthrough. The results of this model confirm that the ^{135}Xe only adds 2.6 W to the average power generated in the bed.

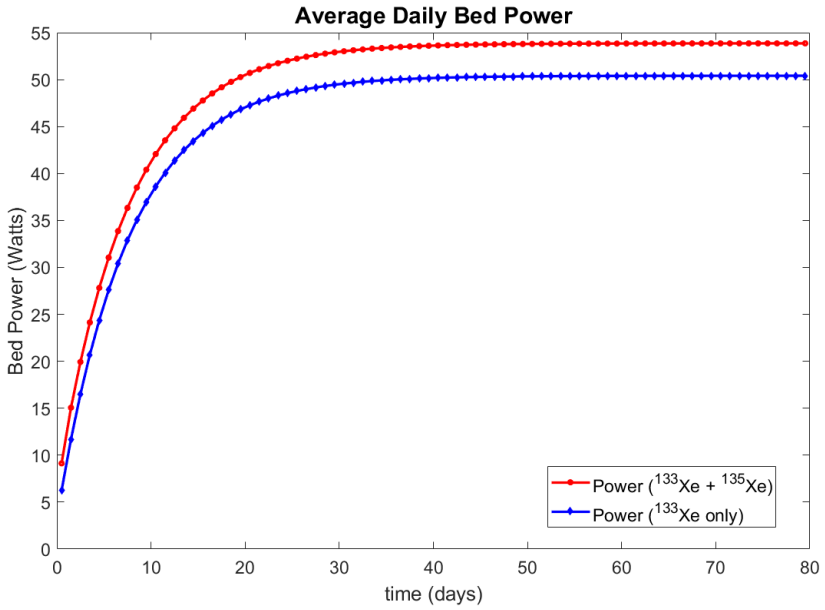

Figure 12. The average daily power (in Watts) produced by radioactive decay in the packed as a function of time (in days). The average daily power is defined as the power generated by radioactive heating in the bed at the midpoint between daily injections.

Pacific Northwest National Laboratory

902 Battelle Boulevard
P.O. Box 999
Richland, WA 99354
1-888-375-PNNL (7665)

www.pnnl.gov